LETTER

doi:10.1038/nature09996

Convergence of electronic bands for high performance bulk thermoelectrics

Yanzhong Pei[1], Xiaoya Shi[2], Aaron LaLonde[1], Heng Wang[1], Lidong Chen[2] & G. Jeffrey Snyder[1]

Thermoelectric generators, which directly convert heat into electricity, have long been relegated to use in space-based or other niche applications, but are now being actively considered for a variety of practical waste heat recovery systems—such as the conversion of car exhaust heat into electricity. Although these devices can be very reliable and compact, the thermoelectric materials themselves are relatively inefficient: to facilitate widespread application, it will be desirable to identify or develop materials that have an intensive thermoelectric materials figure of merit, *zT*, above 1.5 (ref. 1). Many different concepts have been used in the search for new materials with high thermoelectric efficiency, such as the use of nanostructuring to reduce phonon thermal conductivity[2–4], which has led to the investigation of a variety of complex material systems[5]. In this vein, it is well known[6,7] that a high valley degeneracy (typically ≤6 for known thermoelectrics) in the electronic bands is conducive to high *zT*, and this in turn has stimulated attempts to engineer such degeneracy by adopting low-dimensional nanostructures[8–10]. Here we demonstrate that it is possible to direct the convergence of many valleys in a bulk material by tuning the doping and composition. By this route, we achieve a convergence of at least 12 valleys in doped $PbTe_{1-x}Se_x$ alloys, leading to an extraordinary *zT* value of 1.8 at about 850 kelvin. Band engineering to converge the valence (or conduction) bands to achieve high valley degeneracy should be a general strategy in the search for and improvement of bulk thermoelectric materials, because it simultaneously leads to a high Seebeck coefficient and high electrical conductivity.

A high thermoelectric figure of merit, *ZT*, for a high-efficiency thermoelectric generator requires the constituent n-type and p-type materials each to have a high average thermoelectric materials figure of merit, $zT = S^2\sigma T/(\kappa_E+\kappa_L)$, where T, S, σ, κ_E and κ_L are the temperature, Seebeck coefficient, electrical conductivity, and the electronic and lattice components of the thermal conductivity, respectively. To date, commercial products for thermoelectric power generation utilize only PbTe- or Bi_2Te_3-based materials with peak *zT* of less than unity[5].

Recent efforts to raise the *zT* value of PbTe have focused on nanostructured composites, such as $Na_{1-x}Pb_mSb_yTe_{m+2}$ (ref. 3), where the aim is to reduce κ_L and thus to enhance *zT*; indeed $zT > 1$ has been obtained in many instances[2]. Such materials have κ_L close to the amorphous limit[2,4], lending greater potential to the increasing of *zT* by the enhancement of the electronic component ($S^2\sigma$). Seebeck coefficient enhancement through density of states modification[8,11] is a promising route, but this approach risks the reduction of carrier mobility.

The optimal electronic performance of a thermoelectric semiconductor depends primarily on the weighted mobility[6,7,12], $\mu(m^*/m_e)^{3/2}$; here m^* is the density-of-states effective mass, μ is the mobility of carriers, and m_e is the electron mass. However, μ is low for bands with heavy mass m_b^* (the band-mass of a single valley, or mass of a single pocket of Fermi surface related to $1/(d^2E/dk^2)$ of the pocket). In fact, for charge carriers predominantly scattered by acoustic phonons (as has been found to occur in most good thermoelectric materials), it is expected that $\mu \propto 1/m_b^{*5/2}$ (ref. 7). Therefore, increasing the band-mass should be detrimental to the thermoelectric performance[7].

In contrast, the convergence of many charge carrying valleys has virtually no detrimental effects. Multiple degenerate valleys (separate pockets of Fermi surface with the same energy) have the effect of producing large m^* without explicitly reducing μ. A valley degeneracy N_v has the effect of increasing m^* by a factor of $N_v^{2/3}$. Specifically, the density-of-states effective mass used to analyse most thermoelectric data is given by $m^* = N_v^{2/3}m_b^*$ (refs 6, 7, 12, 13), where N_v includes orbital degeneracy, and m_b^* is, more specifically, the average (single valley) density-of-states effective mass of the degenerate valleys (including the effect of spin degeneracy but not orbital degeneracy or degeneracy imposed by the symmetry of the Brillouin zone)[6]. The mobility is nominally unaffected by N_v, but there may be some reduction due to intervalley scattering.

It is thus clear that a large valley degeneracy is good for thermoelectric materials[6,7,12,13]. More generally, bands may be regarded as effectively converged when their energy separation is small (compared with k_BT, where k_B is the Boltzmann constant); this leads to an effective increase in N_v, even when the bands are not exactly degenerate. The concept of carrier pocket engineering to produce convergence (high N_v) of symmetrically inequivalent bands has been suggested in the context of manipulating low-dimensional thermoelectric nanostructures[8–10]. Extending this concept to bulk materials would be most useful for rapid integration into commercial devices.

Convergence of many valleys can occur in high symmetry crystal structures (such as PbTe and $(Bi, Sb)_2Te_3$) if the Fermi surface forms isolated pockets at low symmetry points. The widely used thermoelectric material $(Bi,Sb)_2Te_3$ has significant valley degeneracy, with $N_v = 6$ in both the conduction and valence bands[7]. The valence band extremum in PbTe occurs at the L point in the Brillouin zone, where

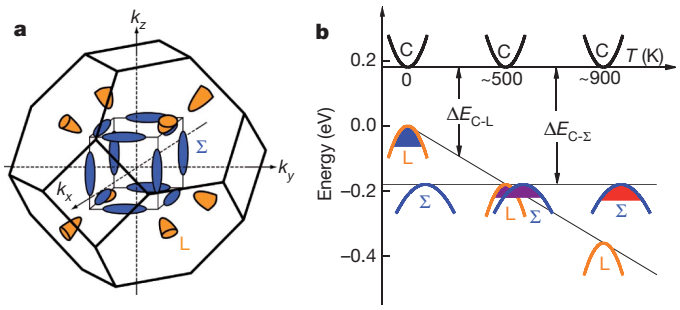

Figure 1 | Valence band structure of $PbTe_{1-x}Se_x$. **a**, Brillouin zone showing the low degeneracy hole pockets (orange) centred at the L point, and the high degeneracy hole pockets (blue) along the Σ line. The figure shows 8 half-pockets at the L point so that the full number of valleys, N_v, is 4, while the valley degeneracy of the Σ band is $N_v = 12$. **b**, Relative energy of the valence bands in $PbTe_{0.85}Se_{0.15}$. At ~500 K the two valence bands converge, resulting in transport contributions from both the L and Σ bands. C, conduction band; *L*, low degeneracy hole band; Σ, high degeneracy hole band.

[1]Materials Science, California Institute of Technology, Pasadena, California 91125, USA. [2]CAS Key Laboratory of Materials for Energy Conversion, Shanghai Institute of Ceramics, Chinese Academy of Sciences, Shanghai 200050, China.

©2011 Macmillan Publishers Limited. All rights reserved

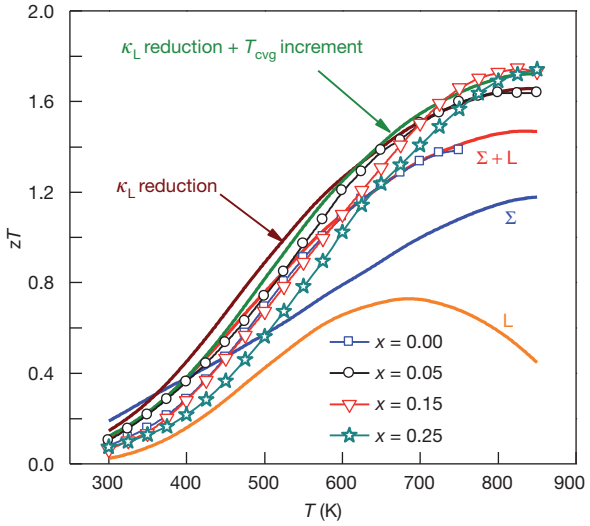

Figure 2 | Temperature dependence of the zT of p-$PbTe_{1-x}Se_x$ materials doped with 2 atom % Na. Symbols are experimental data. Curves are calculated results, based on a three-band model with a total hole density of 2.5×10^{20} cm^{-3}. The zT values calculated for both L and Σ bands (Σ + L) are shown with individual contributions from the L and Σ bands for $x = 0$. The zT for $x = 0.15$ using the predicted κ_L in Fig. 3b is calculated with (κ_L reduction + T_{cvg} increment) and without (κ_L reduction) band structure modification (equation (3)) respectively to compare the individual contributions.

the valley degeneracy is 4 (refs 6,14–16), as in the conduction band of Ge (ref. 17)). However, in addition there is in PbTe a second valence band along the Σ line; this second valence band (the Σ band) has an energy about 0.2 eV below that of the first valence band (the L band), and has a valley degeneracy of 12 (Fig. 1a)[14,15].

By producing the convergence of many valleys at the desired temperatures, thermoelectric performance can be greatly enhanced if properly doped. We demonstrate this effect in $PbTe_{1-x}Se_x$, where the L and Σ valence bands (Fig. 1b) can be converged, giving an increased valley degeneracy of 16. This exceptionally high degeneracy persists to high temperature, at which the effective degeneracy is at least 12 from the Σ band alone. Combining this effect with the low lattice thermal conductivity of $PbTe_{1-x}Se_x$ alloys, we observe a zT value of ~1.8 at temperatures above ~800 K (Fig. 2).

In a system that contains two valence (or conduction) bands, the total electrical conductivity (σ_{total}) and Seebeck coefficient (S_{total}) can be expressed as:

$$\sigma_{total} = \sigma_1 + \sigma_2 \quad (1)$$

$$S_{total} = (\sigma_1 S_1 + \sigma_2 S_2)/\sigma_{total} \quad (2)$$

Here, subscripts 1 and 2 refer to the transport properties of carriers in the individual band. If two bands are present, then the total Seebeck coefficient is a weighted average of the Seebeck coefficients of the individual band; the band with the higher conductivity is more strongly weighted. Because S usually decreases with the number of carriers n, whereas conductivity increases with n ($\sigma = ne\mu$), the total Seebeck coefficient will generally be closer to the smaller S of the two bands. Only when the two band energies are aligned (degenerate), such that the two bands have the same Seebeck coefficient, will S_{total} be maintained while the total conductivity is substantially higher than that of either band alone. In general, this effect will improve thermoelectric performance when the bands are within $\sim 2k_BT$ of each other, owing to the broadening of the Fermi distribution, making band convergence easier to achieve at higher temperatures. Additionally, higher doping concentrations place the Fermi level deeper within the first band, helping to position the Fermi level within $\pm 2k_BT$ of both bands.

The existence of the secondary (Σ) valence band slightly below the principal (L) valence band in PbTe has been confirmed by recent density functional theory calculations[18]. A schematic band structure[15] of PbTe is depicted in Fig. 1b. With this two valence band model, the electrical transport, optical spectroscopy and other properties of p-PbTe can be well understood. Most importantly, the L band moves below the Σ band at $T \gtrsim 450$ K. Temperature (T, in K)-dependent energy offsets (in eV) of the L and Σ bands from the conduction (C) band are given by[14–16,19]:

$$\Delta E_{C\text{-}L} = 0.18 + (4T/10{,}000) - 0.04x$$
$$\Delta E_{C\text{-}\Sigma} = 0.36 + 0.10x \quad (3)$$

where x refers to the subscript x in $PbTe_{1-x}Se_x$. Partial substitution of Se for Te ($PbTe_{1-x}Se_x$) increases the energy of the L band and reduces the energy of the Σ band (resulting in the terms including x in equation (3) above), according to a linear dependence of band energy versus Se content[20]. Therefore, alloying with Se will increase the convergence temperature (T_{cvg}) of the L and Σ bands. Na is an effective p-type dopant in PbTe, and can be used to obtain a hole density above 10^{20} cm^{-3} by replacing nominally divalent Pb with monovalent Na (ref. 21). The valence band at the L point with $N_v = 4$ has sufficient mobility to enable a good zT of about 0.8 (curve 'L' in Fig. 2 is the contribution from the low degeneracy L band, calculated using the model described in Supplementary Information). The second valence band along the Σ line with a higher $N_v = 12$ has even higher performance (curve 'Σ' in Fig. 2) at such doping levels.

When both the L and Σ bands are aligned the carriers are redistributed, populating the highly degenerate Σ valleys, which creates a Seebeck coefficient that increases faster than the typical linear temperature dependence (Fig. 3a). With the combined 16 hole pockets

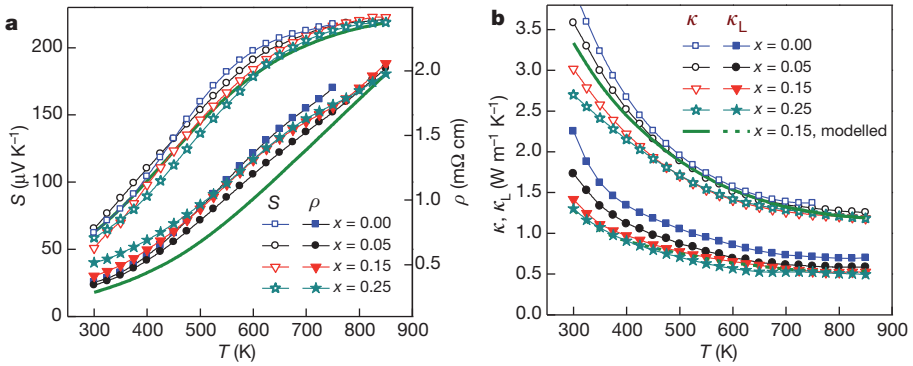

Figure 3 | Thermoelectric transport properties of $PbTe_{1-x}Se_x$ alloy doped with 2 atom % Na. a, Temperature dependence of the Seebeck coefficient S and resistivity ρ. **b**, Total thermal conductivity κ and its lattice component κ_L. The solid green curves show the results of the three-band model and the dashed green curve shows the predicted κ_L according to the Debye–Callaway model for $x = 0.15$ with a hole concentration of 2.5×10^{20} cm^{-3}.

©2011 Macmillan Publishers Limited. All rights reserved

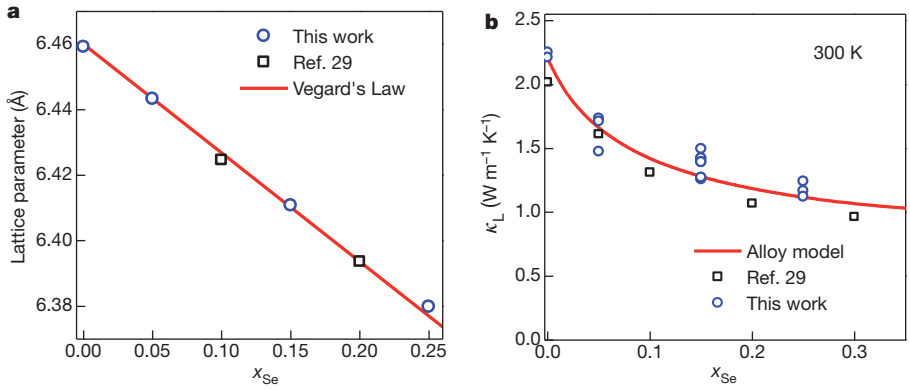

Figure 4 | Composition dependence of lattice parameter and lattice thermal conductivity for $PbTe_{1-x}Se_x$ doped with Na, compared with models expected for alloys. Literature results[29] are included in this figure. **a**, The 300 K lattice parameter obeys Vegard's law, which is expected for a solid solution. **b**, Lattice thermal conductivity can be well described by an alloy scattering model. Multiple data points in **b** are for different samples with the same Se content but with Na doping varying in the range 1–2 atom %.

contributing, a high zT of ~1.3 at ~700 K (for example, curve 'Σ + L' in Fig. 2) can be obtained, similar to that seen in PbTe heavily doped with alkali metals (Na or K)[22,23].

As mentioned above, alloying with Se increases T_{cvg}, further tuning the thermoelectric properties so as to increase the zT in the temperature range for waste heat recovery (400–900 K). The energy difference between the L and Σ bands, $\Delta E_{L-\Sigma}$, of the ($PbTe_{1-x}Se_x$) alloy is reduced to $<\sim 2k_BT$ even at high temperatures, making the two bands effectively converged. Alloying with Se has the extra benefit of increasing the bandgap (helpful for higher temperature operation) and also provides lower lattice thermal conductivity due to point defect scattering of phonons. Further increasing the Se content may improve the peak zT but additional Se leads to lower mobility from impurity scattering of electrons, and therefore no significant benefit in average zT is realized, similar to that found in under-doped alloys[24]

To confirm that the multi-band effects are indeed responsible for the extraordinary thermoelectric properties, we have developed a detailed three-band model (C+L+Σ). It is important to include the temperature dependence of the bandgap, band offsets and effective masses to fit the data accurately. These parameters have been determined by optical absorption spectroscopy and other temperature dependent transport properties for a wide range of carrier densities[14–16,19,25,26]. Bands L and C have been found to be non-parabolic and have been described by the Kane model[14,27], whereas the high degeneracy hole band Σ has been described as parabolic[14,28]. It is also assumed that acoustic phonons dominate the electron scattering[14,27]. This model also gives the Lorenz factor (Supplementary Fig. 3) needed to calculate the electronic contribution to the thermal conductivity. The details of this model are given in Supplementary Information.

The X-ray lattice parameter (Fig. 4a, Supplementary Fig. 1) of our annealed samples follows the simple form of Vegard's law, which predicts a linear change from 6.46 Å for PbTe (ref. 14) to 6.12 Å for PbSe (ref. 14), suggesting the formation of a simple alloy consistent with previous studies[14,29]. Na is also expected to be homogeneously distributed because of the high dopant effectiveness of monovalent (Na^+) on the Pb site (Hall effect data are given in Supplementary Fig. 3), and because there are no trivalent species present to induce clustering as found in some other similar systems[2,3], such as $Na_{1-x}Pb_mSb_yTe_{m+2}$. Nevertheless, we cannot entirely rule out the possibility of some segregation to native defects, nanometre-scale particles, voids or other interfaces that have been proposed to affect thermoelectric properties, including electronic effects such as electron filtering[8]. However, the success of our model in predicting transport properties using only bulk properties (electronic structure, and electron and phonon scattering) shows that nanoscale effects are not necessary to achieve exceptionally high zT in PbTe alloys (Fig. 2, Supplementary Information). Combining this exceptional bulk performance with independent nanoscale effects, such as the scattering of long mean free path phonons by nanostructural interfaces[2–4], would lead to further enhancements of zT, probably giving values above 2, and also improve the average ZT for use in efficient waste heat recovery.

The observed reduction in κ_L as Se content increases (Fig. 4b) is expected from alloys, as phonons are scattered due to the mass difference and local strain caused by the impurity atoms, and can be well characterized by the Debye-Callaway model[4,29] (see Supplementary Information for details). Using the electronic model and the lattice thermal conductivity (κ_L), zT can be calculated at any doping level, alloy composition and temperature.

The temperature dependence of the Seebeck coefficient, the resistivity ($\rho = 1/\sigma$) and the thermal conductivity are shown in Fig. 3. The measured temperature dependent transport properties agree very well with the electronic model, confirming that the exceptional thermoelectric properties arise when the valley degeneracy is large, particularly when the L and Σ bands converge (within $\sim 2k_BT$). Because of the high density-of-states mass (m^*) resulting from the convergence of many (at least 12) valleys, heavy doping is required to realize the full potential of high degeneracy to produce high zT. The zT measured on 2% Na-doped $PbTe_{0.85}Se_{0.15}$ (1.8 ± 0.1 at 850 K, determined on multiple samples on multiple instruments, Supplementary Fig. 2) shows good agreement with the calculated zT, as seen in Fig. 2.

In summary, high valley degeneracy produced by carrier pocket engineering in a bulk material is an effective strategy to enhance thermoelectric performance through the convergence of conducting electronic bands, provided that the doping is properly tuned. Heavily doped p-$PbTe_{1-x}Se_x$ demonstrates how high valley degeneracy enables high zT, especially when combined with other mechanisms (such as alloy scattering) that reduce κ_L. A high zT value of ~1.8 at high temperatures make these simple and stable materials superior to those currently in use for thermoelectric energy generation applications.

METHODS SUMMARY

Polycrystalline $Pb_{0.98}Na_{0.02}Te_{1-x}Se_x$ samples were prepared by melting the mixture of pure elements at 1,273 K, quenching, annealing at ~900 K for 3 days, grinding and hot-pressing (98% or higher relative density). X-ray diffraction and scanning electron microscope analyses confirm that the materials for this study were single phase solid solutions. The Seebeck coefficient was obtained from the slope of the thermovoltage versus temperature gradient, confirmed on four different high temperature systems. Scanning Seebeck coefficient measurements (at 300 K) on a sample with a zT of ~1.8 at 800 K showed a Seebeck coefficient variation of only 5 μV K^{-1} (full width for 90% of the data taken in an area of 6.5 × 7 mm^2). Four-probe resistivity was measured using the Van der Pauw technique on disks, and using the linear method on bar shaped samples. Thermal diffusivity was measured using the laser flash method. Heat capacity (C_p) is estimated from the relation C_p/k_B per atom = $3.07 + (4.7 \times 10^{-4} \times (T - 300))$, where T is in K, based on experimental

©2011 Macmillan Publishers Limited. All rights reserved

literature values[30]. The combined uncertainty for the experimental determination of zT is ~20%; the standard deviation of the measured zT at $T = 800 \pm 50$ K is 4% for four different techniques and 3% for four different samples, all of the same $x = 0.15$ composition. The Hall coefficient at room temperature and higher was measured using the Van der Pauw technique under a reversible magnetic field of ~2 T. The low temperature (2.5–300 K) Hall coefficient was measured using a Quantum Design PPMS.

Received 13 December 2010; accepted 14 March 2011.

1. Bell, L. E. Cooling, heating, generating power, and recovering waste heat with thermoelectric systems. *Science* **321,** 1457–1461 (2008).
2. Kanatzidis, M. G. Nanostructured thermoelectrics: the new paradigm? *Chem. Mater.* **22,** 648–659 (2010).
3. Poudeu, P. F. P. *et al.* High thermoelectric figure of merit and nanostructuring in bulk p-type $Na_{1-x}Pb_mSb_yTe_{m+2}$. *Angew. Chem. Int. Edn* **45,** 3835–3839 (2006).
4. Pei, Y., Lensch-Falk, J., Toberer, E. S., Medlin, D. L. & Snyder, G. J. High thermoelectric performance in PbTe due to large nanoscale Ag_2Te precipitates and La doping. *Adv. Funct. Mater.* **21,** 241–249 (2011).
5. Snyder, G. J. & Toberer, E. S. Complex thermoelectric materials. *Nature Mater.* **7,** 105–114 (2008).
6. Mahan, G. D. in *Solid State Physics* (eds Ehrenreich, H. & Spaepen, F.) Vol. 51, 81–157 (Academic, 1998).
7. Goldsmid, H. J. *Thermoelectric Refrigeration* (Plenum, 1964).
8. Dresselhaus, M. S. *et al.* New directions for low-dimensional thermoelectric materials. *Adv. Mater.* **19,** 1043–1053 (2007).
9. Koga, T., Sun, X., Cronin, S. & Dresselhaus, M. Carrier pocket engineering to design superior thermoelectric materials using GaAs/AlAs superlattices. *Appl. Phys. Lett.* **73,** 2950–2952 (1998).
10. Rabina, O., Lin, Y. & Dresselhaus, M. Anomalously high thermoelectric figure of merit in $Bi_{1-x}Sb_x$ nanowires by carrier pocket alignment. *Appl. Phys. Lett.* **79,** 81–83 (2001).
11. Heremans, J. *et al.* Enhancement of thermoelectric efficiency in PbTe by distortion of the electronic density of states. *Science* **321,** 554–557 (2008).
12. Slack, G. A. in *CRC Handbook of Thermoelectrics* Ch. 34 (ed. Rowe, D. M.) 406–440 (CRC, 1995).
13. DiSalvo, F. J. Thermoelectric cooling and power generation. *Science* **285,** 703–706 (1999).
14. Ravich, Y. I., Efimova, B. A. & Smirnov, I. A. *Semiconducting Lead Chalcogenides* (Plenum, 1970).
15. Nimtz, G. & Schlicht, B. Narrow-gap lead salts. *Springer Tracts Mod. Phys.* **98,** 27–40 (1983).
16. Ravich, Y. I. in *Lead Chalcogenides: Physics and Applications* (ed. Khokhlov, D.) 1–34 (Taylor and Francis, 2003).
17. Ashcroft, N. W. & Mermin, N. D. *Solid State Physics* 570 (Brooks Cole, 1976).
18. Bilc, D. *et al.* Resonant states in the electronic structure of the high performance thermoelectrics $AgPb_mSbTe_{2+m}$: the role of Ag-Sb microstructures. *Phys. Rev. Lett.* **93,** 146403 (2004).
19. Tauber, R. N., Machonis, A. A. & Cadoff, I. B. Thermal and optical energy gaps in PbTe. *J. Appl. Phys.* **37,** 4855–4860 (1966).
20. Strauss, A. J. Metallurgical and electronic properties of $Pb_{1-x}Sn_xTe$, $Pb_{1-x}Sn_xSe$, and other IV–VI alloys. *Trans. Metall. Soc. AIME* **242,** 354–365 (1968).
21. Fritts, R. W. in *Thermoelectric Materials and Devices* (eds Cadoff, I. B. & Miller, E.) 143–162 (Reinhold, 1960).
22. Androulakis, J. *et al.* Thermoelectric enhancement in PbTe with K or Na codoping from tuning the interaction of the light- and heavy-hole valence bands. *Phys. Rev. B* **82,** 115209 (2010).
23. Pei, Y., LaLonde, A., Iwanaga, S. & Snyder, G. J. High thermoelectric figure of merit in heavy-hole dominated PbTe. *Energy Environ. Sci.* doi:10.1039/c0ee00456a (2011).
24. Kudman, I. Thermoelectric properties of p-type PbTe-PbSe alloys. *J. Mater. Sci.* **7,** 1027–1029 (1972).
25. Chernik, I. A., Kaidanov, V. I., Vinogradova, M. I. & Kolomoets, N. V. Investigation of the valence band of lead telluride using transport phenomena. *Sov. Phys. Semicond.* **2,** 645–651 (1968).
26. Lyden, H. A. Temperature dependence of the effective masses in PbTe. *Phys. Rev. A* **135,** A514–A521 (1964).
27. Ravich, Y. I., Efimova, B. A. & Tamarche, V. I. Scattering of current carriers and transport phenomena in lead chalcogenides. 1. Theory. *Phys. Status Solidi B* **43,** 11–33 (1971).
28. Crocker, A. J. & Rogers, L. M. Valence band structure of PbTe. *J. Phys. Coll.* **29,** 129–132 (1968).
29. Alekseeva, G. T., Efimova, B., Ostrovsk, L. M., Serebrya, O. S. & Tsypin, M. Thermal conductivity of solid solutions based on lead telluride. *Sov. Phys. Semicond.* **4,** 1122–1125 (1971).
30. Blachnik, R. & Igel, R. Thermodynamic properties of IV–VI-compounds: leadchalcogenides. *Z. Naturforsch. B* **29,** 625–629 (1974).

Supplementary Information is linked to the online version of the paper at www.nature.com/nature.

Acknowledgements This work was supported by NASA-JPL and the DARPA Nano Materials programme; the work at SIC-CAS was supported by CAS. We thank J.-P. Fleurial, S. Bux, D. Zoltan and F. Harris for measurements of transport properties at NASA's Jet Propulsion Laboratory and at ZT Plus Inc.

Author Contributions Y.P. synthesized the samples, measured the high temperature properties and developed the three-band model; X.S. and L.C. measured the low temperature Hall coefficient and confirmed the high temperature transport properties on some of the samples. A.L. performed the hot pressing; Y.P., X.S., A.L., H.W., L.C. and G.J.S. analysed the experimental data; and Y.P. and G.J.S. wrote and edited the manuscript.

Author Information Reprints and permissions information is available at www.nature.com/reprints. The authors declare no competing financial interests. Readers are welcome to comment on the online version of this article at www.nature.com/nature. Correspondence and requests for materials should be addressed to G.J.S. (jsnyder@caltech.edu).

©2011 Macmillan Publishers Limited. All rights reserved